Stratospheric and Mesospheric Pressure-Temperature Profiles From the Rotational Analysis of CO_2 Lines In ATMOS/ATLAS-l Infrared Solar Occultation Spectra

G. P. Stiller
Institut fur Meteorologic und Klimaforschung
Kernforschungszentrum Karlsruhe und Universität Karlsruhe
Karlsruhe, Germany

M. R. Gunson, L. L. Lowes, M. C. Abrams, O. F. Raper
and C. B. Farmer
Jet Propulsion Laboratory
Pasadena, CA

R. Zander
Institut d'Astrophysique
Université de Liège
B4000 Liège, Belgium

C. P. Rinsland
Atmospheric Sciences Division
NASA Langley Research Center
Hampton, VA

Abstract

A simple, classical, and expedient method for the retrieval of atmospheric pressure-temperature profiles has been applied to the high-resolution infrared solar absorption spectra obtained with the Atmospheric 'I'race Molecule Spectroscopy (ATMOS) instrument. The basis for this method is a rotational analysis of retrieved apparent abundances from CO_2 rovibrational absorption lines, employing existing constituent concentration retrieval software used in the analysis of data returned by ATMOS. Pressure-temperature profiles derived from spectra acquired during the ATLAS-1 Space Shuttle mission of March-April 1992 are quantitatively evaluated and compared with climatological and meteorological data as a means of assessing the validity of this approach.

Introduction

An essential requirement for any space-based limb-viewing remote sensing experiment attempting to characterize the chemical composition of our environment is an accurate knowledge of the observational geometry as well as the physical state of the atmosphere. Orbiting instruments must in general combine geometric information from the spacecraft ephemerides with available meteorological or remotely sensed atmospheric pressure and temperature data.

The Atmospheric Trace Molecule Spectroscopy (ATMOS) Fourier transform spectrometer is one such instrument which is flown on board the Space Shuttle. It operates in the solar occultation mode and obtains broad band high-resolution infrared solar spectra during orbital sunrises and sunsets. These spectra are used to derive the vertical volume mixing ratio profiles of some thirty atmospheric constituents (Farmer, 1987) to assess the composition of the upper atmosphere and to provide a consistent set of geophysical data for validating chemical and dynamical model predictions.

Although methods have been developed to infer atmospheric pressure-temperature profiles from ATMOS spectral data (Rinsland et al., 1992), these have proved sufficiently time consuming and limited by typical computer resources that a simpler approach to improve the speed of computation has been pursued which also expands the spectral information used for improved accuracy. Essentially, we have used successive rotational analyses of a large number of CO_2 absorption lines, based on the retrieved abundance profiles obtained by an 'onion-peeling' algorithm (Norton and Rinsland, 1991), to improve the initial atmospheric pressure-temperature estimates. This approach is not new; it has been employed in the remote sensing of more distant objects such as planets and stars (e.g. Beer and Taylor, 1978; Mitchell et al., 1990) and has also been used in Earth atmosphere applications (Toth, 1977; Gille and House, 1971). It appears to have lost some of its appeal in the light of recent developments of more sophisticated algorithms, but we believe that the approach keeps its virtue of simplicity, speed, directness, and accuracy when based on high quality remote spectroscopic observations.

ATMOS Spectral Data

The results reported in the present paper were derived from spectra recorded during the ATLAS-1 flight on the Space Shuttle Atlantis between March 24 and April 2, 1992. The instrument, described in detail elsewhere (Morse, 1980) is designed to obtain a broad band infrared solar spectrum with an unanodized spectral resolution of 0.01 cm^{-1} every 2.2 sees. This high speed is required to provide a vertical resolution of approximately 3 km during sunrises and sunsets as seen from the, orbiting shuttle platform.

Solar occultation by the Earth's atmosphere during an orbital sunrise or sunset lasts from 1.5 to 2 minutes from the shuttle's typical altitude of 300 km. To meet signal-to-noise and data rate requirements, the 2 to 16pm spectral response of the instrument is limited by

bandpass filters which are narrower than the complete wavelength range; the wavelength regions covered by the optical filters used during the ATLAS-1 mission are listed in Table 1.

In order to obtain optimal signal-to-noise ratios in each bandpass filter without saturating the HgCdTe detector, the ATMOS instrument's field-of-view (FOV) is also selectable. For example, filter #1 spectra with signal-to-noise ratios greater than 200 were obtained using a FOV of 2.77 mrad diameter; for the broader band, shorter wavelength filter #3 spectra, a FOV of 0.97 mrad was used with a concomitant reduction in the signal-to-noise ratios. A high signal-to-noise ratio for the filter #1 spectra was important because of the key atmospheric gases which are measured in this spectral region: among others, spectral features of HNO_3, $ClONO_2$, O_3, and most of the industrial chlorofluorocarbons (CFCs) lie within this filter range.

Before proceeding with the analysis of ATMOS data for atmospheric constituent profiles, two pieces of information are required: an assignment of a tangent pressure (or height) to each spectrum, and a pressure-temperature profile of the atmosphere. In general, it is difficult to obtain accurate and comprehensive pressure and temperature data along the optical path of limb viewing experiments from external sources. Climatological data which are available from the MSISE-90 models (Hedin, 1991) or actual pressure-temperature data from a meteorological source like the National Meteorological Center (NMC, see data description in Gelman, 1991; Finger et al., 1993), are neither accurate enough nor do they cover a sufficient altitude range to preclude the need for ancillary data for the analysis of the spectra from these experiments. This can be critical where the spectral features of interest are temperature sensitive and consequently the temperature profile must be known exceptionally well.

Fortunately, for infrared solar absorption investigations like ATMOS, the viewing geometry or tangent pressure assignment to individual spectra can be retrieved simultaneously with temperature-pressure profile information from the observations themselves. This provides such measurements with a self-contained ability to provide all the necessary information independent of external sources. However, this approach is restricted to spectra in which both temperature insensitive as well as temperature sensitive CO_2 lines are available (Rinsland et al., 1987; Rinsland et al., 1992), such as those obtained with ATMOS filter #3. The temperature insensitive CO_2 lines provide pressure information, while the temperature sensitive CO_2 lines are used to retrieve the tangent height temperatures. Additional information about the tangent pressure can also be obtained from temperature independent , N_2 lines (Demoulin et al., 1992) when these are present in the spectral region covered. Pressure and temperature have been retrieved from the selected CO_2 lines either by applying a global fit approach (Rinsland et al., 1992; Carlotti, 1988), or an onion-peeling approach (Rinsland et al., 1987). In either case, a height scale can be assigned to the retrieved pressure-temperature profile by assuming hydrostatic equilibrium and the absolute value of pressure at one specific height (Gille and House, 1971). At this point, tangent pressure and tangent height can be used interchangeably.

The approach described above does not work in the filter # 1 spectral region of the ATMOS experiment (600 -1180 cm-l), where only very weak temperature insensitive lines covering only a small altitude range, are available. This limits the ability to determine both the tangent pressures for individual spectra and an accurate pressure-temperature profile. In earlier analyses, using temperature-pressure profiles determined from ATMOS filter #3 occultation data coupled to pressure-sensing using the limited number of available $C0_2$ lines from the filter #1 spectral region, the uncertainties in the temperature profiles and the tangent pressures were estimated to produce an error of about 8% in the retrieved volume mixing ratios of molecules such as O_3 (Gunson, et al., 1990). Subsequently, temperature-pressure profiles were retrieved using a global fit algorithm first tested with ATMOS filter #3 spectral data (Rinsland, et al., 1992), but this typically suffered from two practical limitations when applied to filter # 1 observations: it was time-consuming, and its application was restricted by computer memory availability. In consideration of these limitations and the large volume of filter #1 data returned by the ATMOS instrument, we deemed it to be prudent to pursue an alternate approach for assigning accurate tangent pressures to these spectra while simultaneously retrieving the physical state parameters of the atmosphere.

Method Description

In developing a retrieval algorithm, a choice generally has to be made between calculating derivatives either numerically or analytically. The former method tends to be more computation intensive. Furthermore, in complex retrieval problems such as that posed in extracting temperature profiles (as opposed to vmr profiles), numerical approaches are even more time consuming. If an analytical expression can be used, this potentially represents a tremendous saving in computation time.

An "onion-peeling" retrieval algorithm discussed by Norton and Rinsland (1991) has proved to be a reliable and accurate tool for the derivation of concentration profiles of trace gases from the ATMOS observations. In this algorithm a single parameter, a target gas concentration, is iterated in a least squares fashion over a specified altitude range to achieve a fit between an observed and a calculated spectrum within a narrow interval containing an isolated absorption feature. This is relatively quick, but the algorithm was not designed to retrieve pressure and temperature directly.

The approach discussed here assumes a knowledge of the true CO_2 vmr profile. The basic idea of the approach is to retrieve the apparent CO_2 concentrations and use the deviations from the true ones as a function of transition lower state energy as indicators of an erroneously assumed p-T profile. This is achieved by using an iterative procedure based on the onion-peeling algorithm mentioned above. It makes use of the rotational analysis of the lines of several CO_2 bands with a wide range of lower state energies. For this study we have assumed the atmosphere to be horizontally homogeneous and in hydrostatic equilibrium up to about 100 km. Furthermore, we have assumed a global 1992 CO_2 profile as listed in Table 2. CO_2 is assumed to be well mixed at a constant mixing ratio in the stratosphere and mesosphere. Above the mesopause, the atmosphere can no longer be expected to be in

local thermodynamic equilibrium (LTE) and the absorption by CO_2 may no longer be determined by the kinetic temperature alone. Furthermore, the detailed CO_2 profile is not well known above ~80 km, as it reaches the turbopause, where molecular diffusion rates compete with the photolysis of CO_2 in determining its exact vertical profile. Additionally, since the principal objective of the ATMOS experiment is the study of the middle atmosphere, we have focussed on the retrieval of temperatures and pressures at altitudes below 70 km. The lower boundary of the retrieval is determined by the availability of suitable CO_2 lines, a large selection of which can be found down to ~15 km.

In the transmission case, an atmospheric feature can be described by an equation of radiative transfer of the form:

$$I(\upsilon)/I_0(\upsilon) = \exp(-S(T_i) * f(p_i,T_i,\upsilon) * X_i * N_i(p_i,T_i,l_i)) \quad (1)$$

In this expression, the ratio of the atmospheric absorption spectrum $I(\upsilon)$ at the frequency υ to the exe-atmospheric spectrum $1_0(11)$ is the normalized transmittance, $S_.$ is the line intensity, Xi is the volume mixing ratio, N_i is the number density along the optical path in the layer i under consideration, and f is the line shape function. The number density N_i depends on the pressure p_i, temperature T_i and the length of the optical path l_i in the layer i, and can be written as:

$$N_i(p_i,T_i,l_i) = pi/kTi * l_i \quad (2)$$

In the onion-peeling retrieval, only Xi is varied until a fit is achieved between the observed and calculated spectrum. In the process of fitting a spectrum in a constituent retrieval, the volume mixing ratio X_i is varied until a satisfactory agreement between the measured and the calculated spectrum is achieved. Under such a condition the absorption feature calculated at the assumed pressure p' and temperature T' and at the true pressure p and temperature T are effectively indistinguishable, such that:

$$S(T'_i) * X'_i * p'_i/kT'_i * l'_i = S(T_i) * Xi * pi/kTi * l_i \quad (3)$$

where X' is the retrieved CO_2 mixing ratio for the pressure - temperature pair (p', T'). We assume from here on that the difference in the optical paths for the assumed and true p-T model is negligible. This assumption will have consequences on the stability of the retrieval which will be discussed later. The terms for the line shape function have been dropped in equation 3 since they will be effectively equivalent, in particular at the resolution of the ATMOS measurements (0.01 cm^{-1}) and at the altitudes which are of major interest for the ATMOS experiment; below ~18 km, this approximation will no longer be valid (this will also be discussed later in more detail). The line intensity can be more explicitly written as:

$$S(T) = SO * Q_R(T_0)/Q_R(T) * Q_V(T_0)/Q_V(T) * \exp\{hcE''/kT_0 - hcE''/kT\}$$

$$* [1-\exp\{-hc\upsilon/kT\}]/[1-\exp\{-hc\upsilon/kTo\}] \quad (4)$$

where SO is the line intensity at the reference temperature, TO (~296K), Q_R and Q_v are the rotational and vibrational partition sums, respectively, [1-exp{-hcω /kT}] is the spontaneous emission term, and E' is the lower state energy of the transition. The speed of light (c), Boltzman's constant (k), and Planck's constant (h) in this expression will be replaced by the expression for the secondary radiation constant c_2 = 1.438786 K/cm^{-1}. To simplify this expression, we make the assumption that neither the rotational and vibrational partition sums nor the spontaneous emission term changes significantly when we go from the initially assumed temperature T' to the 'true' temperature T in the atmospheric layer under consideration. With this simplification, we can transform equation (2) to:

$$\ln\{X'\} = \ln\{p_i/T_i^* T'_i/p'^*_i \; Xi\} + c_2 * E''*[1/T'_i - 1/T_i] \quad (5)$$

which represents a linear relationship between the log of the retrieved volume mixing ratio from a line and its lower state energy. By evaluating the results of the retrieval of many lines which span a the largest possible range of E", the 'true' temperature T and the 'true' pressure p for this spectrum can be estimated from Equation 5, the latter by using the standard volume mixing ratio profile of CO_2 given in Table 2 for X.

In practice, only transitions of the main isotope $^{12}C^{16}O_2$ were selected to avoid any uncertainty due to the isotopic mixing ratio, particularly at the higher altitudes. No Q branch lines were used, to circumvent any line-mixing effects not included in the forward model calculation of the onion-peeling algorithm, Lines were used for the analysis as soon as they were at least 3 times as strong as the noise level in the spectrum, and they were no longer used when their wings were not free of interference by other lines. We were unable to restrict the selection of lines to weak (unsaturated atmospheric) features, but had to extend the list to include saturated lines in order to cover a sufficiently wide range of lower state energies.

The initial guess p-T profile for the retrieval was a combined model merged from MSISE-90 (Hedin, 1991) and NMC data (Gelman, 1991; Finger, et al., 1993). The MSISE-90 data were used where no NMC data were available, usually above the stratopause. Often the two data sets differed by up to 20 K in the stratopause region. In these cases, an average over the upper range of the NMC levels and the climatological data was used. Initial tangent heights were assigned to the spectra by retrieving them from CO_2 lines in the spectral region from 633 cm^{-1} to 963 cm^{-1} (even though these lines are not temperature insensitive enough to be used in this way), in a manner described by Abrams, et al. (in preparation).

Starting from the initial p-T profile and assigned tangent heights, the retrieval software was used to recover the apparent volume mixing ratio of CO_2 for each single microwindow over the selected altitude range. The results of these retrievals were collected and combined in a plot of ln(X') versus E" for each altitude, and a regression line was fitted to these distributions. For this, each data point was weighted by its standard deviation estimated from the residuals of the non-linear least squares fit algorithm and from the estimation of the signal-to-noise ratio of the spectra; The corrected temperature was derived from the

slope of the regression line. The corrected pressure was derived by comparing the intercept of the regression line with the ordinate axis (the retrieved volume mixing ratio X') to the one of the standard model given in Table 2. The standard deviations of the slope and the intercept of the regression line were calculated, taking into account the weighting of the individual data points by their standard deviation. The standard deviations of pressure and temperature as well as the retrieved volume mixing ratio $(p/p')*X$ (corrected by the temperature error, but not the pressure error) were calculated following a Gaussian error propagation. Within this, the standard deviation of the reference CO_2 profile was assumed to be 1% up to 60 km and 3% above that altitude.

For the second (and subsequent) iterations, an improved physical model was set up from the p-T pairs retrieved from the spectra. The model was extended with MSISE-90 and NMC data at altitudes where no retrieval was possible. Discontinuities occurring at the points where the different models were merged were smoothed by averaging over several points or vertically shifting one of the models. The complete profile was then brought into hydrostatic equilibrium by assuming that the pressure and geometric height of the tropopause were provided correctly by the NMC data. Thus, new tangent heights were calculated from the retrieved p-T pairs for all spectra of the occultation. The next iteration step was then started with the refined physical model and the assigned tangent heights.

In practice, a single, direct calculation of the refined pressure-temperature profile was found to overcorrect the atmospheric p-T profile, and on repeated iterations the solution diverged. A number of approximations are involved in the derivation of equation 5 which are likely to inhibit convergence, one of which is the following: we assume for the calculated corrections that only the tangent layer has a significant impact on the total absorption due to a spectral CO_2 line. However, corrections which are made to higher atmospheric levels will also impact lower layers under consideration, In addition, we assume that the optical path remains unchanged when comparing the absorption signal calculated from the parameters p'_i, T'_i, l'_i, and X'_i to the measured signal determined by the parameters p_i, T_i, l_i, and Xi. By doing this, we' include the correction which would need to be made to l'_i in the correction to p'_i and T'_i. This again results in an over-estimation of the correction to the tangent pressure and temperature. Damping of the calculated corrections in pressure and temperature was necessary because of this over-compensation, which severely decreased the convergence. We found that the calculated corrections in p and T had to be empirically attenuated by 2/3 to improve the convergence.

Results and error analysis

The method described above was applied to all of the available ATMOS/ATLAS-l filter #1 occultations listed in Table 3. Results from the analysis of one filter #3 occultation for comparison with filter #1 occultations obtained at similar latitudes are discussed below.

a) Filter #1 occultations:

In the ATMOS filter #1 spectral region (600 -1180 cm^{-1}), 97 CO_2 lines were found to be useful for the rotational analysis described above. The spectroscopic parameters of all lines were taken from the current updated version of the ATMOS line list (Brown et al., 1987; Brown, private communication, 1993). The assumed CO_2 parameters are the same as in the 1992 HITRAN compilation (Rothman, et al., 1.992). The lower state energies E' of the transitions cover the range from 43 cm^{-1} to 2028 cm^{-1}, and the lines lie within the spectral range from 645.8 to 969.2 cm 1 Each line was selected to be in a microwindow free of absorption lines of other atmospheric constituents, and to represent a single value of E. The frequency of the lines, their lower state energy, and the altitude region they cover for the retrieval are listed in Table 4. An example of the rotational analysis of three different ATMOS-ATLAS-1 spectra assigned to tangent heights of 65.7, 39.0, and 27.2 km from occultation SR37 is shown in Figure 1. These examples show the transition in altitude coverage between lines with different E, with no low E lines available for the lower altitude analyses.

From the slope of these lines it is clear that in each case some correction to the atmospheric temperature profile is needed. Pressure sensing alone, based on the available CO_2 spectral features in this optical band pass, without correction of the temperature clearly leads to erroneous pressure determination. For example, for the CO_2 line at 949.48 cm^{-1} with a lower state energy of 1470 cm^{-1}, typical of the lines in the so-called laser bands which can be used through the stratosphere, a temperature error of 10 K at 260 K corresponds to an error in the retrieved line of sight amount of 22% This is an extreme example but it demonstrates the need for a simultaneous pressure-temperature retrieval.

The left panel of Figure 2 shows the retrieved CO_2 profile after three iteration steps of occultation SR37. The CO_2 profile is corrected by the temperature error but not by the pressure error; i. e., $(p/p')*X$ is plotted. The pressure correction for each spectrum can be derived directly from these profiles. The CO_2 profile resulting from the first retrieval step deviated by as much as 1009Io from the expected CO_2 profile. Generally within three iteration steps the CO_2 concentrations became close enough to the standard profile, as seen in Figure 2, to be acceptable with regard to the error bars, at least for altitudes above 30 km.

Below 30 km, successive iterations beyond the third step did not appear to provide any further improvement in the convergence. There are two likely causes for this behavior, The

first is that in this altitude range, only the strong laser band lines with high lower state energies are available for the p-T retrieval, and these lines become less sensitive to changes in the target gas amount and thus less suitable for any retrieval. They were included in the list of usable lines despite these characteristics only because they were the only available lines in this altitude range. The high lower state energies of these lines makes the extrapolation to the intersection with the ordinate highly uncertain, which causes the calculated pressure to have a relatively large uncertainty. A filter #3 occultation was investigated to check this assumption, since for the spectral region covered there, the distribution of the lower state energies of the available CO_2 lines in Filter #3 is different and more appropriate to the task. These results are reported in Section b) below.

The second probable reason for the recurring oscillations in the retrieved CO_2 profile is the error propagation which is inherent in the onion peeling retrieval method (Carlotti, 1988). We cannot neglect the impact of this because the weighting functions of a limb viewing experiment like ATMOS with successive measurements every 2.5 - 3.5 km overlap significantly. This is further compounded by the finite field of view used in the observations, which is significantly larger than the spacing of the spectra in filter #1 occultations. In general, the ATMOS occultation data readily lend themselves to onion-peeling retrievals and are quite robust in this *sense*, but we still pay a penalty in some error propagation.

The effects due to the weighting function overlap can be reduced by analyzing the spectra individually. Each spectrum was separately fitted by scaling the volume mixing ratio in the tangent layer and the layers above by the same scaling factor, without recourse to onion-peeling. After having retrieved the apparent CO_2 volume mixing ratio for a spectrum at a given tangent height, the CO_2 concentration was reset to the standard value of 347 ppmv and the next lower spectrum was treated in the same way. As shown in the right, panel of Figure 2, the recurring oscillations were removed by decoupling the spectra in this manner during the retrieval, achieving a further convergence in the CO_2 profile with this iteration step.

The p-T profile was considered to be acceptable if a CO_2 mixing ratio profile could be retrieved which was within $\pm$ 5 % of the one listed in Table 2, which is consistent with a *one* sigma error in the retrieved profile. An example of the final retrieved profile is" shown in Figure 3 for the occultation SR37, and compared to the initial NMC and MSISE-90 data. Generally, the retrieved profile is closer to the NMC data than to the MSISE-90 climatological model. The NMC data are based on satellite data and any available radiosonde measurements. Therefore, the NMC data can be expected to be more representative of the prevailing atmospheric conditions.

The 1 sigma standard deviation in the derived profiles is considered to be 0.5-2 K in temperature and 1.5% - 3% in pressure. The altitude region with highest precision is the region between 30 and 60 km. In the altitude region below this, the reduced precision reflects the lack of microwindows with an appropriately distributed temperature sensitivity. Above 60 km, most of the lines which can be used lie in a spectral region where the signal

to noise ratio is low (below '700 cm^{-1}), or the lines are already very weak, and the main uncertainty is due to the relatively high standard deviation in the retrieved vmr values (compare Figure 1). Following the error analysis of Rinsland, et al. (1992) for pressure and temperature retrievals from ATMOS/Spacelab 3 data, we have estimated the overall accuracy of the retrieved pressure-temperature profiles based on separate systematic error sources as listed in Table 5. The root sum square of the systematic and statistical error estimates suggests an overall accuracy of 2 K in temperature and 6% in pressure.

b) Filter #3 occultations

In a way similar to the Filter #1 retrievals, 124 CO_2 lines for the optical filter #3 (1550 - 3350 cm-l) were selected. They cover the spectral region from 1890.3 cm^{-1} to 3325.3 cm^{-1} and their lower state energies range from O to 3048 cm^{-1}. Their frequencies, lower state energies, and the altitude ranges over which they are useful are listed in Table 6. The filter # 3 region has the advantage that for all altitudes, spectral microwindows covering a wide range of lower state energies are available (compare Table 6 with Table 4).. Thus, the spectroscopic information provides more homogeneity in the altitude coverage of temperature sensitive and temperature insensitive lines than in filter #1. Furthermore, the smaller FOV employed in the filter #3 observations may have contributed to reducing the oscillations occurring in the lower altitude range. From this, we conclude that the oscillations occurring in filter #1 occultations are caused by a combination of lines with inappropriate spectroscopic qualities and the onion-peeling error propagation as a result of the overlapping FOV.

The retrieved CO_2 profile for the third iteration step of the filter #3 SR05b occultation is shown in Figure 4. The error bars of the derived CO_2 profiles for filter #3 occultations are in the order of 10%, which is mainly due to the significantly lower signal-to-noise ratio in this filter region. Because of this, the accuracy of the retrieved pressure-temperature profiles is limited to 2-3 K in temperature and to 1096 in pressure. The final pressure-temperature model derived from the retrieval of occultation SR05b is shown in Figure 5 in comparison to the NMC and MSISE-90 data, The agreement between the retrieved filter #3 temperatures and the NMC values is similar to that found with the filter #1 data.

Summary and Conclusions

The ultimate purpose of establishing this method of simultaneously assigning tangent pressures to ATMOS spectra while deriving pressure-temperature profiles is to facilitate an accurate retrieval of constituent profiles from the ATMOS spectral data. A detailed intercomparison of a number of these constituent retrievals with other satellite measurements is underway, to be described in future papers, which will provide validation of this procedure. At this stage it is possible to compare the derived pressure-temperature profile directly with other sources of data. As already recognized by Rinsland, et al (1992), when retrieving pressure-temperature profiles for the ATMOS Spacelab 3 mission in 1985, climatological models are not useful for verifying the quality of the retrieved profiles

because of significant daily and interannual temperature variability. This is reconfirmed when comparing the retrieved profiles with the MSISE-90 data shown in Figures 3 and 5. The model data disagree in the altitude as well as in the temperature of the stratopause, in some cases by up to 12 K. In general, the stratopause is found at a higher altitude in the retrieved profile than in the MSISE-90 profile. The NMC. data in these figures were calculated for the time and the location of the ATMOS occultation (R. Nagatani, private communication). Differences between the retrieved p-T pairs and interpolated NMC data for all available ATMOS/ATLAS-1 occultations are presented in Figure 6. In contrast to the MSISE-90 data, the NMC data agree to better than 5 K at most heights, although larger differences exist at the stratopause, the region of maximum uncertainty in the NMC values. The slight systematic bias between the ATMOS results and the NMC data which can be seen in Figure 6 between pressure levels of 5 and 100 mbars remains unexplained. However, this bias is tolerable with respect to the real use of this data in trace gas retrievals from the ATMOS spectra,

In summary, we have applied this method to Filter #1 and Filter #3 occultations of the ATMOS/ATLAS-1 data set acquired in March-April 1992. The method makes use of the different temperature dependence of CO_2 lines. We retrieve CO_2 volume mixing ratios which are correlated with the lower state energy of the transitions to infer a tangent pressure assignment together with the tangent temperature. A pressure - temperature profile is obtained by applying this process iteratively, which is accurate to 2 K in temperature and to 6% in pressure for the filter #1 observations, and 2-3 K and 10 % for the filter #3 observations. The advantages of the method presented here as compared to the global fit approach used before in the analysis of ATMOS-Spacelab 3 data (Rinsland et al., 1992) are the reduced computing time, the simplicity, and the accuracy. The method provides tangent pressure assignments and pressure-temperature profiles for ATMOS occultation data which significantly improves the accuracy of atmospheric constituent retrievals from this same data.

Acknowledgments

The authors would like to thank R. Nagatani for providing the NMC data used in this work, and the members of the ATMOS Data Processing Team, Tyler Brown, Julie Foster, John Gieselman, and Gindi Lynch, for their work in reducing and analyzing the data. This work was carried out at the Jet Propulsion Laboratory, California Institute of Technology, under contract with the National Aeronautics and Space Administration. One of us (RZ) was partly supported by the Belgian "Global Change Program", managed by the S. P. P. S., Brussels.

References

Beer, R. and F.W. Taylor, The abundance of carbon monoxide in Jupiter, *Astro. J.*, 221, 1100-1109, 1978.

Brown, L.R., C.B. Farmer, C.P. Rinsland, and R.A. Toth, Molecular line parameters for the atmospheric trace molecule spectroscopy experiment, *Appl. Opt.*, 26, 5154-5182, 1987.

Carlotti, M., Global-fit approach to the analysis of limb-scanning atmospheric measurements, *Appl. Opt.;* 27, 3250-3254, 1988.

Demoulin, P., C. B. Farmer, C. P. Rinsland, and R. Zander, Determination of absolute strengths of N_2 quadruple lines from hugh resolution ground-based IR solar observations, *J. Geophys. Res.*, 96, 13003-13008, 1991.

Farmer, C.B., High resolution infrared spectroscopy of the Sun and the Earth's atmosphere from space, *Mikrochim. Acta*, III, 189-214, 1987.

Finger, F. G., M. E. Gelman, J. D. Wild, M. L. Chanin, A. Hauchecorne, A. J. Miller, Evaluation of NMC upper-stratospheric temperature analyses using rocketsonde and lidar data, Bull. Amer. Met. Sot., 74, 789-799, 1993.

Gelman, M. E., Stratospheric monitoring with TOVS data, Paleogeogr. Paleoclimatol. Paleocol. (Global and Planet. Change Section), 90, 75-78, 1991.

Gille, J.C. and F.B. House, On the inversion of limb radiance measurements, I, Temperature and thickness, *J. Atmos. Sci.*, 28, *1427-1442, 1971.*

Gunson, M.R., The Atmospheric Trace Molecule Spectroscopy (ATMOS) Experiment -The ATLAS-1 Mission, SPIE Vol. 1715, Optical Methods in Atmospheric Chemistry, 513-521, 1992,

Gunson, M.R., C.B. Farmer, R.H. Norton, R. Zander, C.P. Rinsland, J.H. Shaw, and B.-C. Gao, Measurements of CH_4, N_2O, CO, H_2O, and O_3 in the middle atmosphere by the Atmospheric Trace Molecule Spectroscopy experiment on Spacelab 3, *J. Geophys. Res.*, 95, D9, 13867-13882, 1990.

Hedin, A. E., Extension of the MSIS thermosphere model into the middle and lower thermosphere, *J. Geophys. Res.*, 96, 1159-1172, 1991.

Mitchell, G.F., J.-P. Maillard, M. Allen, R. Beer, and K. Belcourt, Hot and cold gas toward young stellar objects, *Astrophys. 1,363,554-573,* 1990.

Morse, P.G., Progress report on the ATMOS sensor: Design description and development status, Proc. AIAA Sensor Systems for the 80's Conference, Colorado Springs, Colorado/ December 2-4, 1980.

Norton, R.H., and C.P. Rinsland, ATMOS data processing and science analysis methods, *Appl. Opt.,* 30, 389-400, 1991.

Rinsland, C.P., M.R. Gunson, R. Zander, and M, Lopez-Puertas, Middle and upper atmosphere pressure-temperature profiles and the abundances of CO_2 and CO in the upper atmosphere from ATMOS/Spacelab 3 observations, *J. Geophys. Res.,* 97, *20479-20495, 1992,*

Rinsland, C.P., J. M. Russell III, J.H. Park, and J. Namkung, Retrieval of upper atmosphere pressure-temperature profiles from high resolution solar occultation spectra, NASA Tech. Memo. 89160, NASA Langley Res. Cent., Hampton, VA., 1987. (Available as N87-24858 from Nat]. Tech. Inf. Serv., Springfield, Vs.)

Rothman, L. S., R. R. Gamache, R. H. Tipping, C. P. Rinsland, M. A. H.' Smith, D. C. Benner, V. Malathy DeVi, J.-M. Flaud, C. Camy-Peyret, A. Perrin, A. Goldman, S. T. Massie, L. R. Brown, R. A. Toth, The HITRAN Molecular Database: Editions of 1991 and 1992, *J. Quant. Spectrosc. Radiat. Transfer,* 48, *469-507, 1992.*

Toth, R.A., Temperature sounding from the absorption spectrum of CO_2 at 4.3 μm, *Appl. Opt.,* 16, *2661-2668, 1977.*

Figure Captions

Fig. 1: Rotational analysis of the retrieved vmr from the evaluated CO_2 lines for 3 spectra assigned to tangent heights of *65.7, 39.0,* and 27.2 km (top to bottom) from the ATMOS ATLAS-1 occultation SR37. At lower altitudes, only the lines in the CO_2 laser bands are available, originating from lower state transitions (E) in excess of 1200 cm^{-1}. For the correct pressure and temperature, a horizontal line with an intersection on the ordinate axis of -7.97 (the natural logarithm of 3.47×10^{-4} - the assumed stratospheric vmr for CO_2) is expected from the regression fit,

Fig. 2: The retrieved CO_2 profiles from the ATMOS ATLAS-1 occultation SR37 after the third iteration step (left panel) and fifth iteration steps (right panel). The retrieved profile has been corrected by the temperature error (slope of the regression fits) but not the tangent pressure correction (i.e., p/p' *X, as described in the text). In each panel, the assumed CO_2 distribution (Table 2) is shown as a dashed.

Fig. *3:* The retrieved pressure-temperature profile from the ATMOS/ATLAS-1 SR37 occultation (filter #1) (solid line with error bars). For comparison, the NMC data (dash-dotted line) and the MSISE-90 climatological model (dotted line) are also shown.

Fig. 4: Retrieved CO_2 profile after three iterations of the analysis of the ATMOS ATLAS-1 occultation SR05b (filter #3). The dashed curve represents the assumed CO_2 profile (Table 2).

Fig. 5 The retrieved pressure-temperature profile for the ATMOS ATLAS-1 occultation SR05b (filter #3) (solid line with error bars). The NMC data (dash-dotted line) and the MSISE-90 climatological model (dotted line) are reproduced for comparison.

Fig. 6: Differences between retrieved temperatures from ATMOS ATLAS-1 filter #1 occultations and values interpolated from appropriate NMC data (plotted as NMC minus ATMOS). The dotted lines in the figure mark the mean errors in the NMC temperatures. The NMC tropopause temperatures have errors of typically 7 K.

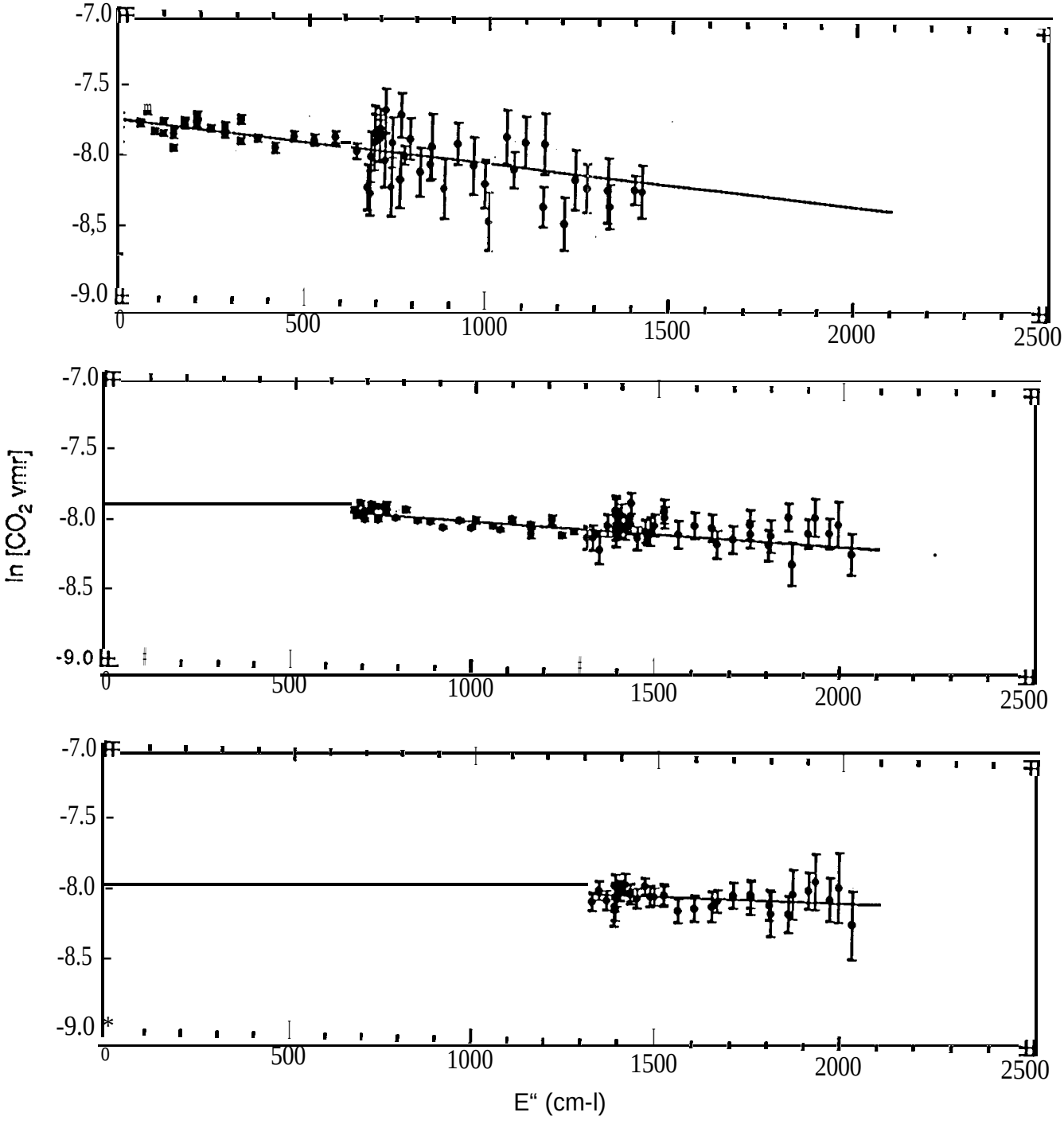

Figure 1.

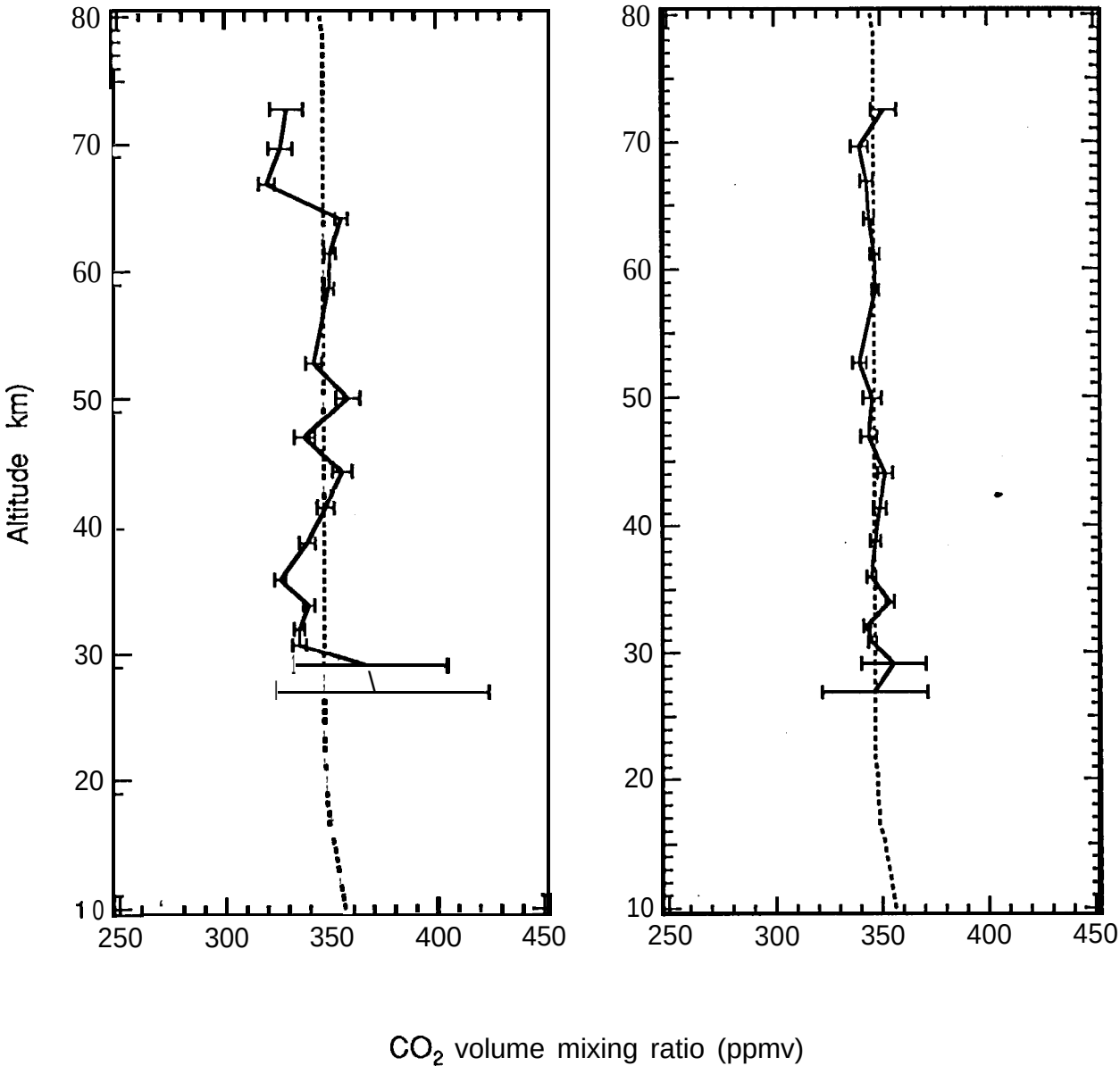
Altitude km)
80
70
60
50
40
30
20
10
250
300
350
400
450
CO_2 volume mixing ratio (ppmv)

Figure 2.

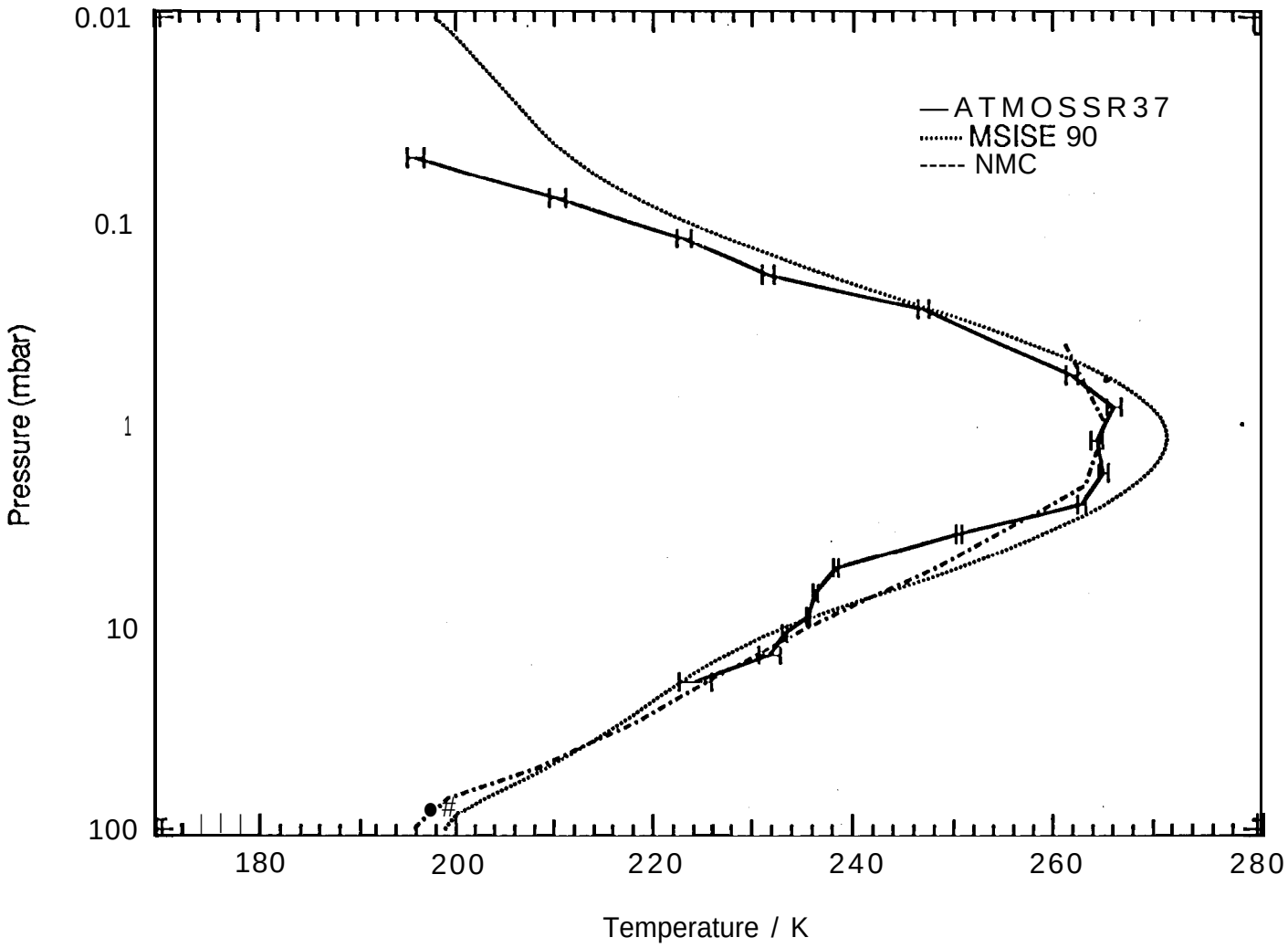
0.01
0.1
1
10
100
Pressure (mbar)
180
200
220
240
260
280
Temperature / K
—ATMOSSR37
MSISE 90
NMC

Figure 3

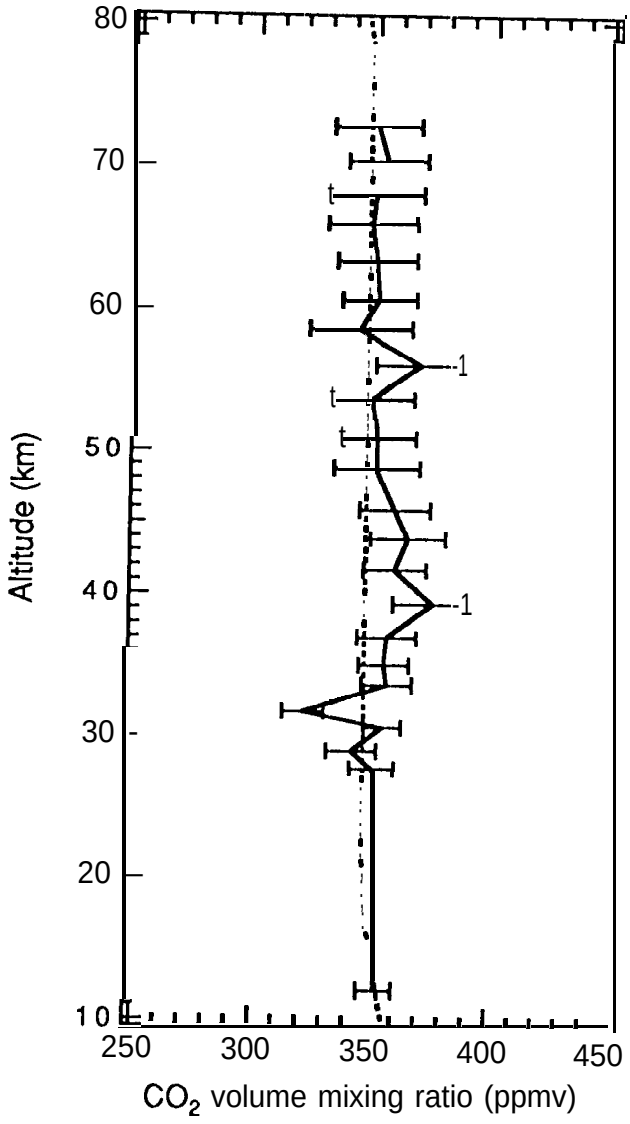
80
70
60
50
40
30
20
10
Altitude (km)
250
300
350
400
450
CO_2 volume mixing ratio (ppmv)

Figure 4

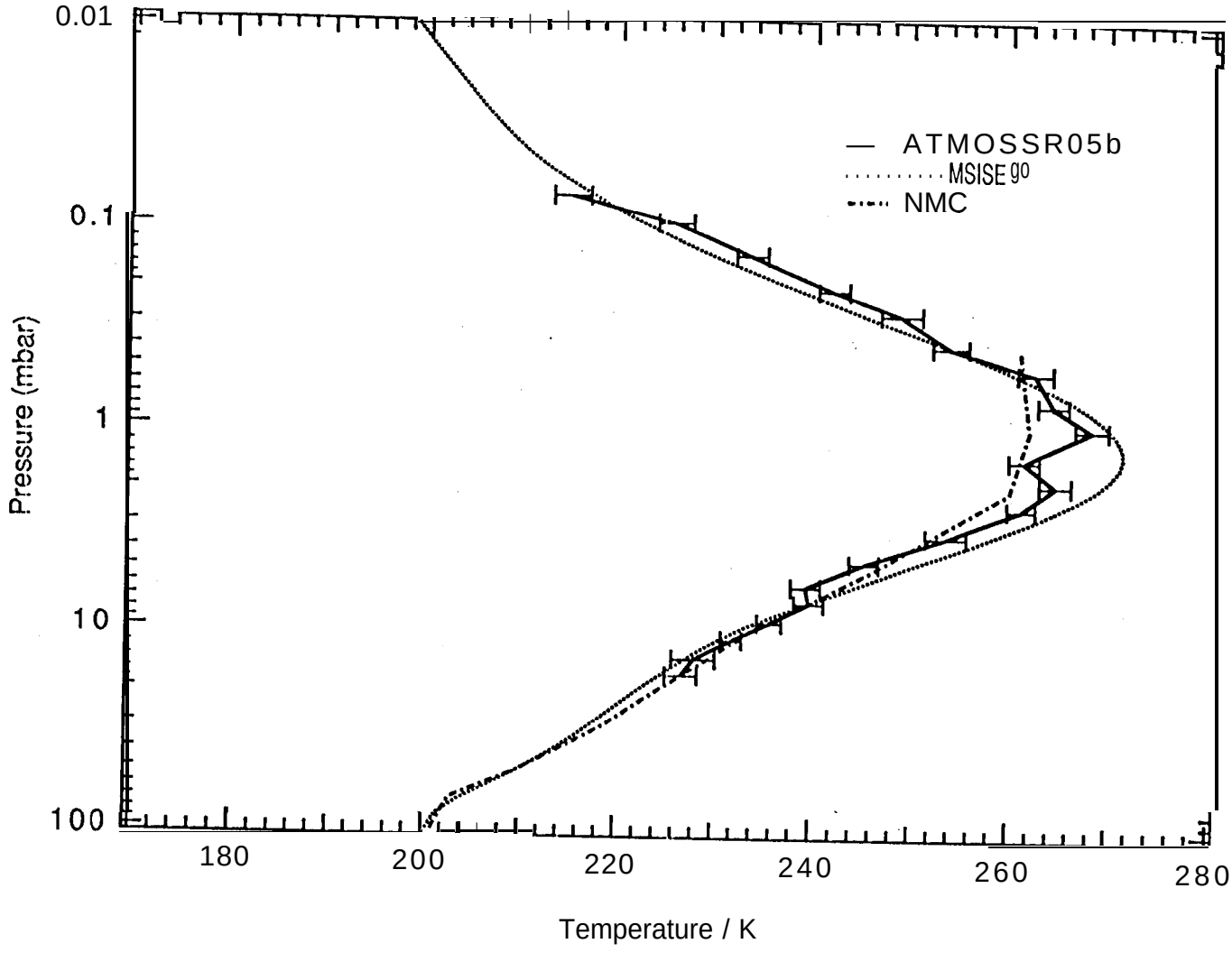
0.01
0.1
1
10
100
Pressure (mbar)
180
200
220
240
260
280
Temperature / K
ATMOSSR05b
MSISE 90
NMC

Figure 5

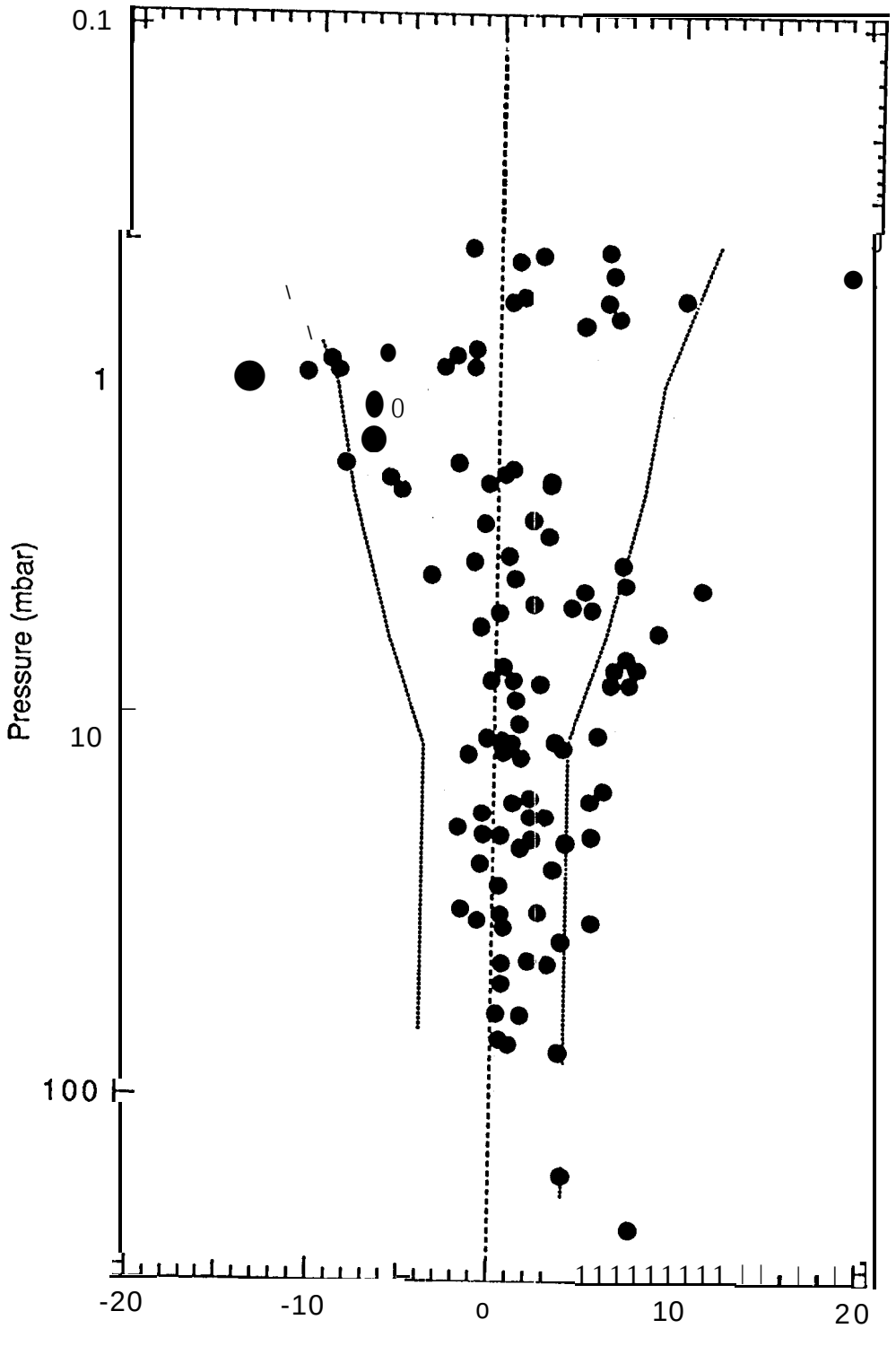
0.1
1
10
100
Pressure (mbar)
-20
-10
0
10
20
Temperature difference (NMC - ATMOS) in deg. kelvin

Figure 6

TABLE 1. ATMOS broad bandpass filters

Filter #	spectral range (cm^{-1})
1	600-1180
2	1100-2000
3	1550-3350
4	3150-4800
9	600-2450

TABLE 2. C02 standard volume mixing ratio profile for 1992 used for the pressure correction in these analyses

Altitude (km)	CO_2 vmr (ppmv)
O-6	360
6-8	359
8-9	358
9-1o	357
10-11	356
11-12	355
12-13	354
13-14	353
14-15	352
15-16	351
16-18	349
18-21	348
21-79	347
79-80	346
80-81	345
81-82	344
82-83	343
83-84	341
84-85	339
85-86	337
86-87	335
87-88	332
88-89	328
89-90	3 2 5

Table 3. ATMOS ATLAS-1 solar occultations made with optical filter #1.

Event Number	Date 1992	UT[1]	Lat.[1]	Long.[1]
SR03	March 25	1007:01	28.4S	300.7E
SR09	March 26	1748:38	17.6S	185.0E
SR26	March 28	1635:18	0.0N	202.4E
SR31	March 29	0008:54	2.6N	88.8E
SS25	March 29	0108:10	46.5S	240.5E
SS26	March 29	1139:49	47.9s	92.2E
SR35	March 29	1512:53	8.0N	222,4E
SR37	March 29	1814:02	9.0N	177.0E
SS31	March 29	2213:28	49.3s	293.4E
SR44	March 30	1520:23	15.4N	219.8E
SS37	March 30	1918:45	51.3s	236.3E
SS43	April 1	0857:21	54.4s	130.0E
SS48	April 2	0131:10	55.3s	240.9E

1. Time, latitude and longitude are given for each observation closest to measurements at a tangent height of 30 km.

TABLE 4. Microwindows used in the rotational analysis in the filter # 1 spectral range

Central frequency (cm-1)	Width (cm-1)	E" (cm-1)	Altitude range (km)
645.86	0.20	316.77	80 - 54
647.37	0.20	273.87	80-54
650.41	0.20	197.42	80-52
651.90	0.20	163.87	80-56
653.46	0.20	133.44	80-58
655.00	0.20	106.13	80-58
656.53	0.20	81.94	80-56
658.07	0.20	60.87	80-56
659.61	0.20	42.92	80-56
680.77	0.20	106,13	110-56
682.36	0.20	133,44	110-56
683.96	0.20	163.87	110-56
685.55	0.20	197,42	110 -56
687.15	0.20	234.08	110 -56
688,76	0.20	273.87	106 -56
690.36	0,20	316.77	106-54
691.97	0.20	362.79	106 -54
693.58	0.20	411,92	106-54
695.20	0.20	464.17	102-54
696.82	0.20	519,54	100 -52
698.44	0.20	578,01	98-50
700.06	0.20	639.60	93-50
701.68	0.20	704.30	75-47
703.31	0.20	772.11	91-47
704.94	0,20	843.03	91-45
706.58	0.20	917.06	86-30
708.21	0.20	994.19	86-30
708.99	0.20	761.12	86-30
709.85	0.20	1074,43	86-30
710.58	0.20	738.47	84-33
711.49	0.20	1157.77	84-33
712.16	0.20	718.94	84-33
713.13	0,20	1244.22	84-33
713.74	0.20	702.54	84-33
714.78	0.20	1333.77	84-33
715.32	0.20	689.26	84-33
716.43	0.20	1426.42	84-33
716.89	0.20	679.10	84-33
723.92	0.20	672.07	82-31
725.47	0.20	679.01	82-31
727.02	0.20	689.26	84-31
728.57	0,20	702.54	86-31
730.11	0,20	718,94	86-30
731,65	0.20	738.47	86-30
733.18	0.20	761,13	86-30
734.71	0.20	786.90	86-30
736.24	0.20	815,80	86-30
737.76	0.20	847.83	86-30

TABLE 4. (Continued).

Central frequency (cm^{-1})	Width (cm^{-1})	E" (cm^{-1})	Altitude range (km)
739.28	0.20	882,97	86 - 30
742.32	0.20	962.63	82-30
743.83	0.20	1007.13	82-30
745.34	0.20	1054,76	77-30
746.84	0.20	1105.51	77-30
748.34	0.20	1159.37	75-30
749.84	0.20	1216,35	73-30
751.34	0.20	1276.45	73-28
752.83	0.20	1339.66	70-28
754.32	0.20	1405.98	68-28
755.81	0.20	1475.42	65-28
798.47	0.08	1313.52	55-30
800.03	0.20	1328.36	60-13
801,59	0.20	1346,32	63-13
803.14	0.20	1367.40	60-15
804,70	0,20	1391.61	58-25
809.37	0.20	1482.95	56-12
810.93	0.20	1519.64	60-10
812.48	0.20	1559.45	60-10
814.04	0.20	1602.38	56-10
815,60	0.20	1648.42	56-10
818.71	0.20	1749.86	54-11
820.27	0.20	1805.25	52-8
821.83	0.20	1863.76	50-12
823.39	0.20	1925.37	50-12
824.95	0.20	1990.11	47-12
924.97	0.20	2,027.79	47-15
927.01	0.20	1966,19	47-10
929.02	0.20	1907.71	47-8
931.00	0.20	1852.35	47-8
932.96	0.20	1800.09	47-8
934.89	0.20	1750.96	52-10
936.80	0.20	1704.94	52 - 10
938.69	0.20	1662.04	52-10
945,98	0.20	1521.62	56-13
947.74	0.20	1494.31	56-20
949.48	0.20	1470.12	56-13
951.19	0.20	1449,05	56-14
952.88	0.20	1431.10	56-14
954.55	0,20	1416.28	54-14
956.19	0.20	1404.57	54-1o
957.80	0.30	1395.99	50-8
959.39	0.30	1390.53	45-10
961.73	0.30	1388.18	45-8
963.26	0.30	1390.53	50-8
964.77	0.20	1395.99	54-11
966.25	0.20	1404.57	54-13
967.70	0.20	1416.28	56-15
969,14	0.20	1431.10	56-15

TABLE 5, Sources and impact of systematic errors (1 sigma)

Source of error	Estimated error	Resulting error in: Pressure (%)	Temperature (K)
C02 line intensities	2 %	1-2%	0.2 K
C02 line widths and air-broadening coeff. (below 30 km)	3%	o-1 %	0.4 K
temperature dependence of the C02 line widths (below 30 km)	10%	o-1 %	0.3 K
C02 profile	1-3%	1-3 %	OK
zero level offset and normalization the spectra	2 %	o-2 %	< 1 K
root sum square		< 5 %	< 1 K

TABLE 6. Microwindows used in the rotational analysis in the filter # 3 spectral range (1550 -3350 cd).

Central frequency (cm- 1)	Width ((.$_m$- 1)	E“ (cm^{-1})	Altitude range (km)
1890,33	0.30	1244.22	50-12
1893.25	0.30	10'74.43	56-12
1896.17	0.30	917,06	52-12
1897.64	0.30	843.03	52-21
1899.11	0.30	772.11	55-21
1900.59	0.30	704,30	58-21
1902.07	0.30	639.60	58-21
1903.55	0.30	578.01	58-24
1905.04	0.30	519.54	62-25
1906.53	0.30	464.17	63-25
1909.50	0.30	362.79	63-27
1911.00	0.30	316.77	65-27
1912.52	0.30	273.87	65-27
1914.03	0.30	234.08	65-27
1915.55	0.30	197.43	65-27
1917.06	0.30	163.87	64-28
1918.58	0.30	133,44	63-28
1920.11	0.30	106.13	63-28
1921,64	0.30	81.94	66-30
1924.71	0.30	42.92	64-27
1926,26	0.30	28.10	60-30
1927.80	0.30	16.39	60-27
1929.35	0.30	7.80	55-23
1930,91	0.30	2.34	42-21
1936.39	0.30	7.80	47-21
1937.96	0.30	16.39	47-21
1939.54	0.30	28.10	42-21
1941.12	0.30	42,92	40-18
1949.09	0.30	163,87	36-14
1950.70	0.60	197.42	42-18
1952,31	0.30	234,08	42-21
1953.92	0.30	273.87	42-20
1955,54	0.30	316.77	45-18
1957.15	0.30	362.79	44-21
1958,78	0.30	411.92	48-21
1960.40	0.30	464.17	48-21
1962.03	0.30	519.54	42-18
1963.66	0,30	578.01	45-18
1965.29	0.30	639.60	48-21
1966,92	0.30	704.30	46-15
1968.56	0.30	772.11	42-12
1970.20	0.30	843,03	40-12
1971.84	0.30	91”1.06	36-12
1975,13	0.30	1074.43	33-12
1976.78	0.30	1157.77	31-12
2032,41	0.30	1333.77	55-30

Table 6. (Continued).

Central frequency (cm^{-1})	Width (cm^{-1})	E" (cm^{-1})	Altitude range (km)
2036.91	0.30	1074.43	59-30
2038.41	0.30	994.19	60-35
2039.92	0.30	917.06	60-30
2041.44	0.30	843,03	65-33
2042,95	0.30	772,11	65-33
2044.47	0.30	704.30	68-33
2045.99	0.30	639.60	68-33
2047.51	0.30	578.01	70-35
2049.04	0.30	519.54	72-44
2050.57	0,30	464.17	75-38
2052,09	0.30	411.92	75-42
2053.56	0.30	1744,64	75-44
2055.16	0.30	316.77	80-44
2056.70	0.30	273.87	80-38
2058.24	0.30	234.08	80-44
2059.78	0.30	197.42	80-44
2061.32	0.30	163.87	80-48
2062,87	0.30	133,44	80-50
2065.97	0.30	81.94	80-50
2067.52	0.30	60.87	80-52
2069.07	0.30	42,92	80-52
2070.62	0,30	28.10	80-52
2072.18	0.30	16.39	78-52
2082.33	0.20	16.39	78-54
2083.90	0.20	28.10	70-42
2313.16	0.20	639.60	120-65
2314.58	0.20	186,27	98-60
2315.48	0.20	170.08	95-70
2316.62	0.20	307.35	80-60
2345.98	0.20	7,80	125-70
2381,62	0.30	1074.43	105-65
2382.50	0.30	1157.77	100-65
2383.36	0.30	1244,22	95-60
2384.99	0.30	1426.42	87-55
2385.77	0.30	1522.16	85-55
2386.53	0.30	1621.00	82-52
2387.26	0.30	1722.94	77-50
2387.96	0.30	1827.97	77-47
2388.64	0.30	1936.10	73-44
2389.29	0.30	2047.31	73-40
2389.92	0.30	2161.61	65-35
2390,52	0.30	2279.00	63-30
2391.10	0.30	2399,47	61-30
2391.65	0.30	2523.02	61-25
2392.18	0.30	2649,66	61-25
2392.67	0,30	2779.37	55-20
2393.15	0.30	2912.16	50-20
2393.60	0.30	3048,02	50-20
2412.47	0.30	1449.38	25-15

Table 6. (Continued).

Central frequency (cm- 1)	Width (cm- 1)	E“ (cm- 1)	Altitude range (km)
2416,06	0.30	1391.61	25-15
2421.26	0.30	1328,36	25-15
2615.72	0.30	0.74	27-15
2616.45	0.30	2,21	27-15
2617.18	0.30	4.42	27-15
2620.11	0.30	20.62	27-15
2621.56	0.30	33.14	27-15
3201.48	0.40	234.08	36-12
3203.12	0.40	2,73.87	36-12
3204.76	0.40	316.77	36-12
3206.41	0.40	362.79	36-12
3208.07	0.40	411.92	36-12
3211.38	0.40	519.54	30-12
3213.05	0.40	S78.01	30-12
3299.93	0.40	994.19	33-12
3301.52	0.40	917.06	33-12
3304.71	0.40	772.11	35-12
3306,29	0.40	-/04.30	45-15
3307.88	0.40	639.60	42-15
3309.46	0.40	578.01	42-18
3311.05	0.40	519.54	46-20
3312.63	0.40	464,17	42-20
3314.21	0.40	411.92	45-20
3315.79	0.35	362.79	46-21
3318.95	0.30	273.87	42-20
3320.53	0.30	234.08	45-22
3322.11	0.30	197.42	45-21
3323.68	0.40	163.87	38-18
3325,25	0.40	133.44	38-20